

# Efficient Variation-Aware EM-Semiconductor Coupled Solver for the TSV Structures in 3D IC

Yuanzhe Xu<sup>†\*</sup>, Wenjian Yu<sup>‡</sup>, Quan Chen<sup>†\*</sup>, Lijun Jiang<sup>†\*</sup>, Ngai Wong<sup>†\*</sup>

<sup>†\*</sup>Department of Electrical and Electronic Engineering, The University of Hong Kong, Pokfulam Road, Hong Kong  
Email: {yzxu,quanchen,ljiang,nwong}@eee.hku.hk

<sup>‡</sup>Department of Computer Science and Technology, Tsinghua University, Beijing 100084, China  
Email: yu-wj@tsinghua.edu.cn

**Abstract**—In this paper, we present a variational electromagnetic-semiconductor coupled solver to assess the impacts of process variations on the 3D integrated circuit (3D IC) on-chip structures. The solver employs the finite volume method (FVM) to handle a system of equation considering both the full-wave electromagnetic effects and semiconductor effects. With a smart geometrical variation model for the FVM discretization, the solver is able to handle both small-size or large-size variations. Moreover, a weighted principle factor analysis (wPFA) technique is presented to reduce the random variables in both electromagnetic and semiconductor regions, and the spectral stochastic collocation method (SSCM) [10] is used to generate the quadratic statistical model. Numerical results validate the accuracy and efficiency of this solver in dealing with process variations in hybrid material through-silicon via (TSV) structures.

## I. INTRODUCTION

Driven by the pressing need to increase both performance and functionality while reducing power and cost, 3D stacking integrated circuit (IC) technology is developed and considered as an important potential way to continue the Moore's law. In the 3D IC, through-silicon via (TSV) technique is well developed and widely used to transmit clock, power and signal [1]. To form a TSV, additional mechanical and chemical fabrication processes are required, however, which will inevitably give rise to various process variations, e.g., the surface roughness on the inside walls of the via hole and the fluctuation in doping profile of semiconductor area etc. In literature, various works have been conducted either from the variational aspect of interconnect analysis or device simulation [2]–[6]. However, they are based on the “standalone” simulation framework, which characterizes the metallic interconnects and semiconductor carrier transport mechanism separately. Hence, to assess the uncertainties of hybrid metal-semiconductor structures (e.g., the metal-semiconductor contacts and the TSV structures penetrating different material layers), the traditional de-coupled solver will become insufficient to accurately capture the interactions between different materials.

To deal with these problems, a 3D coupled simulator based on finite volume method (FVM) was developed in [7], [8] to combine the full-wave EM models and semiconductor models, and it is particularly suitable in solving the field problem of TSV structures which consists of a mixture of different materials (metal, insulator and semiconductor). Moreover, a variational A-V solver [9] was proposed recently, which simultaneously solves the Maxwell's equations and the semiconductor drift-diffusion equations in the frequency domain while utilizes the spectral stochastic collocation method (SSCM) [10] to generate the quadratic statistical model. This work aims

to improve the method in [9] with a more feasible process variation model and efficient statistical technique to analyze the TSV structures in 3D IC.

Regarding the modeling of process variations, a smart geometrical model, inspired by [3], is presented to collaborate with the FVM in the coupled A-V solver. It relieves the trade-off between mesh size and deviation magnitude to extend the capability of the variational solver. Furthermore, instead of traditional principle factor analysis (PFA), the weighted PFA (wPFA) [4] is presented to reduce the random variables for both geometrical and material variations. Combined with the sparse grid technique based SSCM, the computational time of statistical analysis is remarkably reduced. Two TSV structures in 3D IC are analyzed to evaluate the combined impact of geometric variations of interconnect and random doping profile (RDF) variation, on the electric current and capacitance quantities. With the comparison with 10000-run Monte-Carlo (MC) simulation, the numerical results demonstrate the accuracy and efficiency of the variational simulator in analyzing the complex hybrid configuration of the TSV structures in 3D IC.

## II. BACKGROUND

### A. Standard A-V solver for coupled EM-semiconductor simulation

The equation system of the A-V solver consists of three parts. Firstly, Gauss's law equation (for semiconductors and insulators) and current-continuity equation (for metals) are used to determine the electric potential  $V$ , which reads

$$\begin{cases} \nabla \cdot [\varepsilon_r(\nabla V + j\omega \mathbf{A})] + \rho = 0, \\ \nabla \cdot [(\sigma_c + j\omega \varepsilon_r)(\nabla V + j\omega \mathbf{A})] = 0, \end{cases} \quad (1)$$

where  $\varepsilon_r$ ,  $\sigma_c$ ,  $\omega$  and  $\rho$  denote the relative permittivity, conductivity, frequency and free charge density, respectively. And,  $\mathbf{A}$  is the vector magnetic potential. Secondly, current-continuity equation is applied to solve for the charge carrier density  $n$  and  $p$  in the semiconductors

$$\nabla \cdot \mathbf{J}_{n,p} + j\omega \rho = \pm U(n, p), \quad (2)$$

where  $U$  is the generation/recombination rate of charge carriers, and  $\mathbf{J}_{n,p}$  stands for the semiconductor current density with  $n$  or  $p$  charge carrier. Thirdly, the modified Ampere's equation is adopted to calculate magnetic potential  $\mathbf{A}$

$$\nabla \times \left( \frac{1}{\mu_r} \nabla \times \mathbf{A} \right) + K(\sigma_c + j\omega \varepsilon_r)(\nabla V + j\omega \mathbf{A}) - K \mathbf{J}_{\text{diff}} = 0, \quad (3)$$

where  $K$  and  $\mu_r$  denote the scaling constant [8] and the relative permeability, respectively.  $\mathbf{J}_{\text{diff}}$  is the diffusion current density.

Based on (1), (2) and (3), a nonlinear system is set up for the unknowns  $\{V, n, p, \mathbf{A}\}$ . With the FVM discretization, the structure is meshed into cubes and variables are assigned to the nodes and links of computational grid. Specifically, scalar potential  $V$  and density variables like  $n$  and  $p$  are associated to the vertices of cells; vector potential  $\mathbf{A}$  are assigned to the centers of links; flux variables are represented as vectors on dual links orthogonally passing through surface centers. Then, a system of nonlinear discretized equations are formed and finally solved with the Newton-Raphson method. For more details we refer the readers to [7], [8], [11].

### B. Stochastic spectral collocation method

The stochastic spectral collocation method (SSCM) [10] is employed in the statistical part of variational A-V solver. Generally, the SSCM method consists of three steps. Firstly, with the utility of principle factor analysis (PFA) technique, the correlated variations are de-correlated and reduced into a smaller set of independent variables. Then, we expand the unknown vector  $[x] = \{V, n, p, \mathbf{A}\}$  into polynomial form as

$$\mathbf{x}(\vec{\zeta}) = \sum_{|i|=0}^{\infty} \vec{x}_{i_1, \dots, i_D} H_{i_1, \dots, i_D}^D(\vec{\zeta}), \quad (4)$$

where  $H_{i_1, \dots, i_D}^D(\vec{\zeta}) = H_{i_1}^1 \times \dots \times H_{i_D}^1$  denotes the  $D$ -dimensional Hermite polynomial of order  $|i| = i_1 + \dots + i_D$  (up to second order in this paper), and  $H_{i_j}^1$  is the one-dimensional orthogonal Hermite polynomial of order  $i_j$ .  $\vec{x}_{i_1, \dots, i_D}$  is the unknown coefficient to be calculated by Gauss-Hermite quadrature. Finally, multiple collocation points are chosen through sparse grid technique to determine the unknown coefficients  $\vec{x}_{i_1, \dots, i_D}$  through multi-dimensional quadrature. In the post-processing, the resultant coefficient  $\vec{x}_{i_1, \dots, i_D}$  enables the calculation of common statistical quantities, e.g., mean and variance,

$$\begin{aligned} [\bar{x}] &= \vec{x}_{0, \dots, 0}, \\ \text{Var}([x]) &= \sum_{i=1}^M \vec{x}_{i_1, \dots, i_D}^2 \langle (H_{i_1, \dots, i_D})^2 \rangle, \end{aligned} \quad (5)$$

where  $\langle (H_{i_1, \dots, i_D})^2 \rangle$  is the inner product of  $H_{i_1, \dots, i_D}$  with the Gaussian PDF of  $\vec{\zeta}$ . In SSCM, PFA decreases the dimension of  $\vec{\zeta}$ . If there is  $d$  variables in  $\vec{\zeta}$ , the sparse grid technique generates  $2d^2 + 3d + 1$  sample points. For each sample, a deterministic structure is solved. Therefore, the number of independent variables is crucial to the computational cost for generating the quadratic statistical model.

## III. EFFICIENT VARIATIONAL COUPLED EM-SEMICONDUCTOR SOLVER

In this section, we present the efficient techniques employed in the variational Coupled EM-semiconductor solver.

### A. A smart geometrical variation model for surface roughness

In [9], the involvement of geometrical process variations will lead to a direct perturbation over the coordinates and the nodes are supposed to randomly fluctuate between their upper and lower neighbor nodes. However, when the fluctuation becomes larger, it is highly possible for a node to exceed the

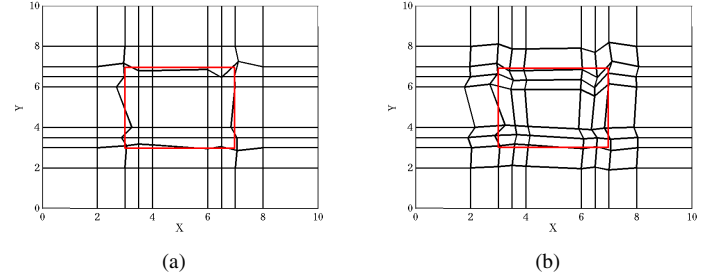


Fig. 1. (a) Simulated cross-section of surface roughness on the inside walls of a TSV structure based on tradition model. The red square stands for the nominal cross-section of a TSV. (b) Simulated cross-section of surface roughness on the inside walls of a TSV structure based on the new geometrical model.

upper or lower boundary, which will lead to the destruction of mesh and the error of calculation (see the perturbed node adjacent to the top right corner of red square in Fig. 1(a)). To avoid this problem, one remedy is to control the deviation setting while enlarging the mesh size of each grid. However, for the sake of accuracy, usually the mesh near the contact will be denser due to the high occurrence of physical interactions there. Consequently, it becomes a trade-off between the simulation accuracy and the functional capability which limits the variational solver in dealing with large-size process variations.

A continuous surface variation (CSV) model was proposed for the boundary element method (BEM) based variational capacitance extraction [3]. It guarantees the smooth connection between surfaces around the aris, in the variational geometry. Facing similar problems in the FVM Cartesian mesh, we are inspired to extend it for the variational A-V solver. The idea is to propagate the interface perturbation to its neighbors along the fluctuating direction, hence all the nodes will fluctuate continuously and the possible overlapping can be avoided. The whole simulated domain can be classified into two parts, one is the inner space enclosed by the perturbed interfaces and the other part is the outer space expanding to the domain boundary. For the inner part, the influences from both interfaces are necessarily taken into account by using a difference propagation equation which reads

$$\xi_i = \xi_r \frac{x_r - x_i}{x_r - x_l} + \xi_l \frac{x_i - x_l}{x_r - x_l}, \quad (6)$$

where  $\xi_i$  denotes the derived variation over the node  $i$ ,  $\xi_r$  and  $\xi_l$  are the random variations on the right and left surfaces, which are generated with the multivariate Gaussian distribution.

For the nodes on the outer side of interface, they are only affected by the nearby interface. We employ another propagation equation for the outer nodes which is denoted as

$$\xi_i = \xi_{l,r} \frac{b - x_i}{b - x_{l,r}} \quad (7)$$

where the  $b$  is the coordinate of the simulation domain boundary,  $\xi_{l,r}$  and  $x_{l,r}$  are the random variation and coordinate on the left or right surface, respectively.

As seen from Fig. 1(b), though more nodes are perturbed continuously due to the propagation formulation, they will not

result in extra computation complexities and errors. Actually, in this simulation approach, different material domains are only defined via the nodes on the material interface, which means only the perturbed nodes on the interface can re-define the physical shape and affect the final results.

### B. Generation and solution of variational matrix equation

Due to the geometrical perturbation we brought into the mesh, the original standard cubes become irregular and the geometrical parameters (e.g. link length, surface area, dual surface and dual volume) change correspondingly. We have proposed techniques to calculate the differential operators [9], and finally a system of nonlinear equations are generated. With the Newton-Raphson method, the following linear matrix equation is to be solved:

$$\begin{bmatrix} \frac{\partial \mathbf{F}}{\partial V} & \frac{\partial \mathbf{F}}{\partial \{p,n\}} & \frac{\partial \mathbf{F}}{\partial \mathbf{A}} \\ \frac{\partial \mathbf{K}}{\partial V} & \frac{\partial \mathbf{K}}{\partial \{p,n\}} & \frac{\partial \mathbf{K}}{\partial \mathbf{A}} \\ \frac{\partial \mathbf{G}}{\partial V} & \frac{\partial \mathbf{G}}{\partial \{p,n\}} & \frac{\partial \mathbf{G}}{\partial \mathbf{A}} \end{bmatrix} \begin{bmatrix} \delta V \\ \delta \{p,n\} \\ \delta \mathbf{A} \end{bmatrix} = \begin{bmatrix} \mathbf{F}(V, \{p,n\}, \mathbf{A}) \\ \mathbf{K}(V, \{p,n\}, \mathbf{A}) \\ \mathbf{G}(V, \{p,n\}, \mathbf{A}) \end{bmatrix} \quad (8)$$

where the derivative matrix on the left hand side is the Jacobian matrix.

### C. Variable reduction with the wPFA technique

Inspired by [3], the weighted principle factor analysis (wPFA) technique is used to replace the traditional PFA technique for variable reduction. The wPFA technique is more efficient due to the utility of an additional weighted function matrix derived from the nominal solution. In detail, the weight function matrix  $\mathbf{W}$  is a diagonal matrix whose elements is the charge quantity on each surface panel in the problem of capacitance extraction. Since they contribute to the resultant parameter under analysis (i.e. the charge of conductor), it is natural to regard the panel charge of nominal structure to the influential factor of the geometrical variation of the corresponding panel.

For the coupled-domain solver, the parameter under analysis is the electric current in the semiconductor domain. In order to reduce the random variables reflecting the doping density, it is reasonable to construct the weight matrix to reflect the current density of nominal structure. The diagonal element of  $\mathbf{W}$  is:

$$w_i = J_{0_i} \cdot \text{node}V_i, \quad (9)$$

where the  $J_{0_i}$  and  $\text{node}V_i$  are the nominal value of current density and space volume of node  $i$ . Then, the weight matrix is multiplied to the covariance matrix whose result is decomposed with the singular value decomposition (SVD). This produces in a matrix  $\mathbf{U}$  of size  $n \times p$ , where  $n$  and  $p$  are the numbers of correlated and reduced independent variables, respectively. Finally, the random geometrical perturbation vector  $\vec{\xi}$  can be obtained with

$$\vec{\xi} = \mathbf{W}^{-1} \mathbf{U} \vec{\zeta}, \quad (10)$$

where  $\vec{\zeta}$  is the truncated set of  $d$ -dimensional independent random variables. Subsequently, the SSCM will accomplish the left steps as introduced in Section II.B.

## IV. NUMERICAL RESULTS

The variational simulation techniques are implemented in MATLAB. A commercial 3D coupled EM-semiconductor sim-

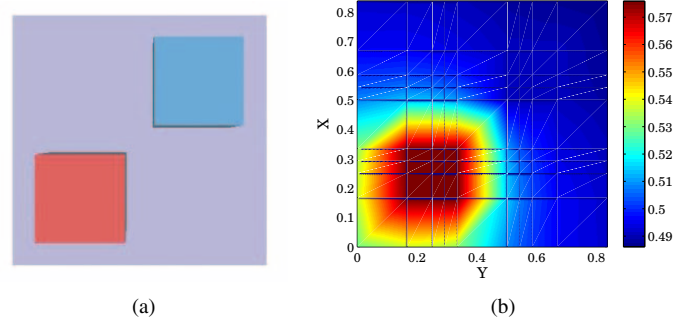


Fig. 2. (a) Top view of two metalplugs sitting on doped silicon (purple is semiconductor, blue is metal and insulator is invisible). This mesh contains 1300 nodes and 3540 links. (b) Cross-section view of the simulation result of electrical field ( $V$ ) on the interface between metalplugs and doped silicon.

ulator from MAGWEL [12] is used as the benchmark, which also generates the nominal geometry mesh. In this section, two hybrid-material structures are tested to validate the presented techniques in analyzing the process variations occurring in the complex configurations. Since large-size process variations are able to be analyzed with the new geometrical model, a more reasonable geometry mesh for the FVM is employed in the simulation.

### A. A hybrid metal-semiconductor structure

The first example is a hybrid material structure with two  $3\mu\text{m} \times 3\mu\text{m} \times 5\mu\text{m}$  metalplugs sitting on a doped silicon which is  $10\mu\text{m} \times 10\mu\text{m} \times 10\mu\text{m}$  (see Fig. 2(a)). In this example, geometrical variations and material (doping) variations are simultaneously incorporated to assess their impacts on the current flowing through the metal-semiconductor interface at  $10^9\text{Hz}$ . A 10% perturbation  $\sigma_M$  is added to the original uniformly distributed doping profile and  $\sigma_G = 0.50\mu\text{m}$  geometrical variations are placed on the metal-semiconductor interface (much larger than the mesh size). There are 32 perturbed nodes on the two rough interfaces with  $\eta = 0.7\mu\text{m}$ , and 72 nodes to model the random doping profile (RDF) effects with  $\eta = 0.5\mu\text{m}$ . The utility of wPFA plays a significant role in reducing the original sets from 32 and 72 to 12 and 10, respectively. Finally, the total 22 independent variables result in 1035 runs of sample structures. The results are listed in TABLE I and the simulation result of electrical field ( $V$ ) is shown in Fig. 2(b).

TABLE I  
CURRENT DENSITY ( $\mathbf{J}$ ) PASSING THROUGH THE  
METAL-SEMICONDUCTOR INTERFACE WITH SURFACE ROUGHNESS AND  
RDF EFFECTS [ $\mu\text{A}$ ]

deterministic	Variation $\sigma_G$ $\sigma_M$	Statistical Indicator	Variational A-V solver+MC	Variational A-V solver+SSCM
0.0078	$\sigma_G \neq 0$	mean	0.0089	0.0089
	$\sigma_M = 0$	std( $10^{-4}$ )	7.9023	7.9078
	$\sigma_G = 0$	mean	0.0082	0.0083
	$\sigma_M \neq 0$	std( $10^{-4}$ )	2.8987	2.9031
	$\sigma_G \neq 0$	mean	0.0087	0.0087
	$\sigma_M \neq 0$	std( $10^{-4}$ )	6.2227	6.2308

Our results are compared with the 10000-run Monte Carlo (MC) simulation. From Table I we can see that the errors on

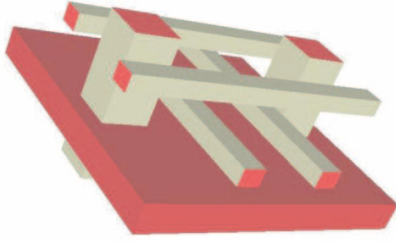


Fig. 3. A TSV test case (metal is in gray, semiconductor is in red, and dielectric is invisible). The mesh contains 4032 nodes and 11332 links.

mean value and standard deviation (std) are both less than 1%. And, the speedup ratio to the MC simulation is about 10X.

### B. A TSV structure in 3D IC

The second example is to analyze the impacts of process variations on the capacitive property of a TSV-based structure. The tested structure includes two TSVs going through a silicon substrate and two metal layers. The TSV has a cross section of  $5\mu\text{m} \times 5\mu\text{m}$  and a height of  $20\mu\text{m}$ . The pitch between TSVs is  $10\mu\text{m}$  and the thickness of silicon substrate and the metal layer are respectively  $5\mu\text{m}$  and  $2\mu\text{m}$ . For the metal traces surrounding TSVs, their width, height and pitch are  $1\mu\text{m}$ ,  $2\mu\text{m}$  and  $2\mu\text{m}$  respectively (see Fig. 3). Based on this hybrid metal-semiconductor structure, the surface roughness on the lateral walls of TSV and the RDF effects in the silicon substrate are considered. Regarding the modeling of surface roughness, we divide the perturbed nodes into 8 groups (each TSV has 4 facets and there are 2 TSVs in total) where the nodes are correlated locally, and there are 64 correlated nodes on each lateral surface. Moreover, if two surfaces from different TSVs lie in the same plane, it is more reasonable to merge them into a larger group with 128 correlated nodes. On the other hand, variations in doping profile are also incorporated into 128 nodes with a 10% perturbation and  $\eta = 0.5\mu\text{m}$  correlation length. Finally, the wPFA reduces the number of random variables from 128 and 64 to 6 and 4, respectively. In total, there are 34 independent variables (resulting from 2 large groups, 4 small groups and 1 doping group) after reduction which leads to 2415 runs of sample structure. The results are shown in TABLE II, where  $C_{T1}$  denotes the self capacitance of the TSV1 on the left,  $C_{T1T2}$  is the coupling capacitance between TSV1 and TSV2 and  $C_{T1W1}$  is the mutual capacitance between TSV1 and wire1, and so on. The results demonstrates the good accuracy of the wPFA based SSCM compared with MC benchmark (with error less than 1%). They also suggest that the variation is very prominent for the TSV capacitances.

### V. CONCLUSION AND FUTURE WORK

In this paper, an efficient variation-aware coupled EM-semiconductor simulation approach is presented to investigate the impacts of process variations on the TSV structure of 3D ICs. Based on the variational A-V solver, various types of variations are incorporated and analyzed simultaneously, which include geometrical variation on the metal-semiconductor interfaces or material variation in doped semi-

TABLE II  
VARIATIONAL ANALYSIS FOR THE CAPACITANCE EXTRACTION OF TSV  
STRUCTURE WITH SURFACE ROUGHNESS + RDF EFFECTS [ $10^{-15}\text{F}$ ]

	Variational		
	A-V solver+MC	A-V solver+SSCM	
$C_{T1}$	mean	7.0567	7.0535
	std	0.8514	0.8577
$C_{T1T2}$	mean	-1.9691	-1.9683
	std	0.4782	0.4769
$C_{T1W1}$	mean	-1.6275	-1.6269
	std	0.3984	0.3972
$C_{T1W2}$	mean	-0.0152	-0.0151
	std	0.00217	0.00212
$C_{T1W3}$	mean	-1.8313	-1.8317
	std	0.1609	0.1709
$C_{T1W4}$	mean	-1.8310	-1.8307
	std	0.1589	0.1593

conductor. A new geometrical model is utilized to extend the capability of existing solver to large-size process variations, and a wPFA technique is presented to dramatically reduce the computational load for statistical analysis.

Due to the complexity of the hybrid nonlinear equation system, the current variational solver still cost several hours to simulate a typical structure. In the future, we will improve it further with the parallel computing technique and a new equation formulation in [11].

### VI. ACKNOWLEDGEMENT

This work is supported in part by NSFC under Grant 61076034 and in part by the Hong Kong Research Grants Council under GRF project HKU 718711E.

### REFERENCES

- [1] A. Papanikolaou and D. Soudris, *Three Dimensional System integration*. New York, NY 10013, USA: Springer, 2011.
- [2] T. El-Moselhy, I. M. Eifadel, and B. Dewey, "An efficient resistance sensitivity extraction algorithm for conductors of arbitrary shapes," *ACM/IEEE DAC*, pp. 84–89, July 2009.
- [3] W. Yu, C. Hu, and W. Zhang, "Parallel statistical capacitance extraction of on-chip interconnects with an improved geometric variation model," in *Proc. IEEE ASP-DAC*, pp. 67–72, 2011.
- [4] —, "Variational capacitance extraction of on-chip interconnects based on continuous surface model," in *Proc. IEEE DAC*, pp. 758–763, 2009.
- [5] Q. Chen, H. W. Choi, and N. Wong, "Robust simulation methodology for surface roughness loss in interconnect and package modelings," *IEEE Trans CAD*, vol. 28, no. 11, pp. 1654–1665, 2009.
- [6] K. Takeuchi and A. Nishida, "Random Fluctuations in scaled MOS devices," in *Proc. IEEE SISPAD*, pp. 1–7, 2009.
- [7] P. Meuris, W. Schoenmaker, and W. Magnus, "Strategy for electromagnetic interconnect modeling," *IEEE Trans CAD*, vol. 20, no. 6, pp. 753–762, June 2001.
- [8] W. Schoenmaker and P. Meuris, "Electromagnetic interconnects and passives modeling: Software implementation issues," *IEEE Trans CAD*, vol. 21, no. 5, pp. 534–543, May 2002.
- [9] Y. Xu, Q. Chen, L. Jiang, and N. Wong, "Process-variation-aware electromagnetic-semiconductor coupled simulation," in *Proc. IEEE IS-CAS*, pp. 2853 – 2856, 2011.
- [10] H. Zhu, X. Zeng, W. Cai, J. Xue, and D. Zhou, "A sparse grid based spectral stochastic collocation method for variations-aware capacitance extraction of interconnects under nanometer process technology," in *Proc. IEEE DATE*, pp. 1–6, 2007.
- [11] Q. Chen, W. Schoenmaker, P. Meuris, and N. Wong, "An effective formulation of coupled electromagnetic-tcad simulation for extremely high frequency onward," *IEEE Trans CAD*, vol. 30, no. 6, pp. 866–876, 2011.
- [12] [Online]. Available: <http://www.magwel.com/>